

RSC Advances



This is an *Accepted Manuscript*, which has been through the Royal Society of Chemistry peer review process and has been accepted for publication.

Accepted Manuscripts are published online shortly after acceptance, before technical editing, formatting and proof reading. Using this free service, authors can make their results available to the community, in citable form, before we publish the edited article. This *Accepted Manuscript* will be replaced by the edited, formatted and paginated article as soon as this is available.

You can find more information about *Accepted Manuscripts* in the [Information for Authors](#).

Please note that technical editing may introduce minor changes to the text and/or graphics, which may alter content. The journal's standard [Terms & Conditions](#) and the [Ethical guidelines](#) still apply. In no event shall the Royal Society of Chemistry be held responsible for any errors or omissions in this *Accepted Manuscript* or any consequences arising from the use of any information it contains.

1 Effect of Aminopropylisobutyl Polyhedral
2 Oligomeric Silsesquioxane Functionalized
3 Graphene on the Thermal Conductivity and
4 Electrical Insulation Properties of Epoxy
5 Composites

6 Peisong Zong^a, Jifang Fu^{*1}, Liya Chen¹, Jintao Yin^{1, 2}, Xing Dong¹, Shuai Yuan¹, Liyi Shi¹ and
7 Wei Deng³

8 ¹ Nano-Science & Technology Research Center, Shanghai University, 99 Shangda Road,
9 Shanghai 200444, PR China

10 ² Department of Chemistry, College of Science, Shanghai University, 99 Shangda Road,
11 Shanghai 200444, PR China

12 ³ School of Chemical and Environmental Engineering, Shanghai Institute of Technology,
13 Shanghai, 201418, P. R. China.

14

15 ABSTRACT

16 In order to obtain homogeneous dispersion and strong interfacial interaction in epoxy
17 nanocomposites, an effective approach is proposed to prepare aminopropylisobutyl
18 polyhedral oligomeric silsesquioxane (ApPOSS) covalently grafted graphene
19 (ApPOSS-graphene) enhancement epoxy (EP) hybrids with high thermal conductivity and
20 electrical insulating property. The chemically converted ApPOSS-graphene 2D sheet with

* Address correspondence to: fjshu@hotmail.com or fjshu@shu.edu.cn (JF Fu)

1 amine groups and rigid Si-O-Si cages is a versatile starting platform to prepare nanohybrids,
2 which conduce to uniform dispersion and well compatibility of graphene in polymer matrix.
3 Compared to pristine GO/EP, the interfacial interactions between ApPOSS-graphene and
4 epoxy matrix through non-covalent and covalent bonds promote well dispersibility,
5 compatibility and interfacial quality in composites, which contribute to improving thermal
6 conductivity through forming effective heat conduct networks and decreasing thermal
7 interfacial resistance. With the incorporation of only 0.25 and 0.5 wt% ApPOSS-graphene,
8 the thermal conductivities of the ApPOSS-graphene/EP composites increase by 37.6% and
9 57.9% compared with neat EP, while maintaining high electrical resistivity. We believe that
10 using ApPOSS chemically reducing and functionalized modifying GO may open a novel
11 interface design strategy for extending applications of POSS and GO to fabricate high
12 performance composites with high thermally conductive and electrically insulating
13 properties.

14 **KEYWORDS:** graphene oxide (GO), polyhedral oligomeric silsesquioxane (POSS), thermal
15 conductivity, epoxy resins

16

17 1. INTRODUCTION

18 Epoxy resins (EPs) are widely utilized at the forefront of many engineering applications,
19 including electronics, automotive, aerospace industry and coatings.^{1,2} However, the generally
20 used EPs are brittle due to its high crosslink density, which restricts their applications. With
21 the rapid development of semiconductors and highly integrated circuit technology, highly
22 thermally conductive and electrically insulative thermal interface materials are increasingly

1 required. Numerous investigations have been performed to explore the high-performance
2 epoxy composites,³⁻⁵ such as mixing epoxy polymers with a second phase of superior
3 nanofillers to enhance the thermal conductivity, thermal stability, mechanical properties, etc.
4 In most of the earlier reports, the addition of Al₂O₃, BN, Si₃N₄ and carbon tubes into the
5 epoxy resin have improved the thermally conductive or electrical insulation because of the
6 intrinsic chemical construction of these additives.⁵⁻⁷ However, in order to obtain high thermal
7 conductivity, the high filler loading content results in destruction in mechanical properties
8 and electrical insulation of the composites.

9 Recently, graphene has aroused extensive interest not only in common scientific studies⁸⁻¹⁰
10 but also in potential applications¹¹⁻¹³ in industrial fields due to extraordinary thermal,
11 electronic, optical and mechanical properties,^{14, 15} which also make it ideal candidate
12 fabricate high performance polymer composites.¹⁶⁻²⁰ However, the graphene sheets are easy
13 to aggregate, which result from Van der Waals and π - π stacking interactions among individual
14 graphene sheets. In addition, the pristine graphene sheets have poor solubility and weak
15 reactivity, which seriously hinder the development of graphene matrix composites. Therefore,
16 a well organic compatibility is important for filler to improve the performance of composite
17 materials. Recent studies have shown that oxygen-containing groups (e.g., -OH, -COOH and
18 epoxy) of graphene oxide grafting organic moieties to get organic soluble graphene is an
19 effective way to satisfy the needs of the applications mentioned above.

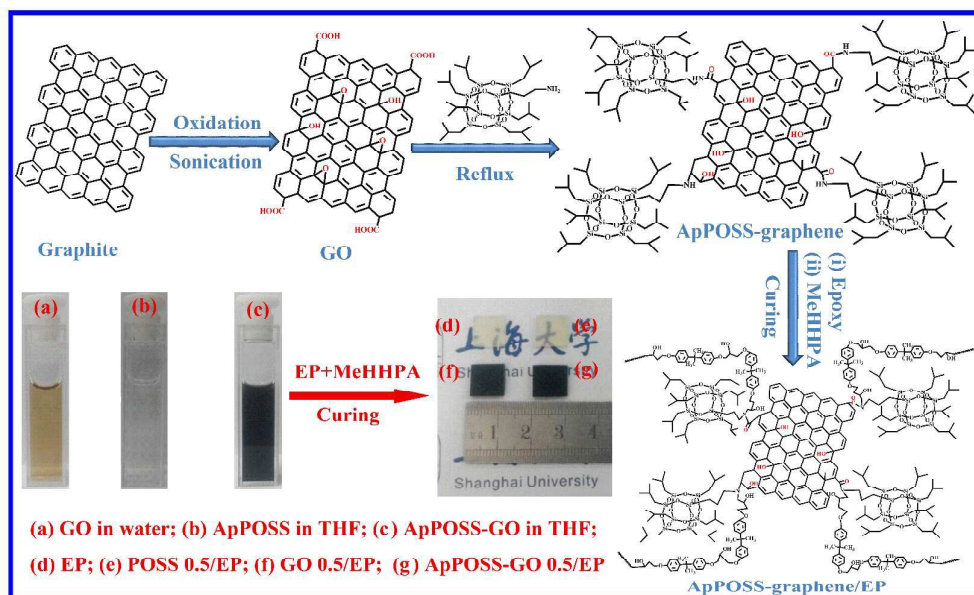
20 Polyhedral oligomeric silsesquioxanes (POSS) are multifunctional materials based on
21 cubic Si-O-Si cage with organic corner pendant groups²¹ that are able to undergo
22 polymerization, grafting or crosslinking.^{22, 23} Their organic-inorganic unique structures endow

1 well compatibility and reactive activity, making it not only effective reinforcement in
2 polymer composites, but also an effective surface modification reagent in nanomaterials.^{24,25}
3 POSS can be incorporated into epoxy networks to improve thermal properties and
4 flammability retardancy of EP composites. It was considered an effective way to improve
5 graphene sheets dispersion and compatibility in polymer composites through covalently
6 modifying graphene oxide with POSS.^{24,26,27}

7 In this work, taking the advantages of the unique structures and properties of POSS and
8 GO, we develop a facile approach to obtain chemically converted aminopropylsobutyl
9 polyhedral oligomeric silsesquioxane (ApPOSS)-graphene nanomaterials enhanced epoxy
10 composites with high thermal conductivity and electrical insulation. GO was covalently
11 functionalized and reduced by aminopropylsobutyl POSS through amide formation between
12 amine of ApPOSS and epoxy or COOH groups of GO (scheme 1). The ApPOSS grafted on
13 GO sheets acts as intercalator between GO interlayers to prohibit the aggregation and
14 restacking the GO sheets in the polymer matrix, at same time, serves as active sites linking
15 graphene sheets and epoxy chains, resulting in significantly improving GO dispersion and
16 compatibility in matrix compared to pristine GO. ApPOSS-graphene sheet as a facile filler
17 has 2D nano sheet structure, which is beneficial to formation of thermal conductive path.
18 Moreover, the well-defined rigid cube Si-O-Si structures contribute to maintaining high
19 electrical insulation and thermal stability. Accordingly, a series of ApPOSS-graphene
20 modified epoxy nanocomposites were prepared, and the effects of ApPOSS-graphene on the
21 chemical microstructure, thermal conductivity, electrical insulation and thermal stability of
22 epoxy nanocomposites were investigated. This investigation may lead to a novel and efficient

1 method to achieve thermally conductive and electrical insulation epoxy composites.

2



4 Scheme 1. Schematic representation of the synthetic route from graphite to
 5 ApPOSS-graphene and ApPOSS-graphene/EP, and photographic images manifested the
 6 dispersion of samples in solvent and cured EP nanocomposites.

7

8 2. EXPERIMENTAL SECTION

9 2.1. Chemical materials

10 Nature Graphite powders were purchased from Qingdao Haida Graphite Co., Ltd (China).

11 Aminopropylisobutyl polyhedral oligomeric silsesquioxane (ApPOSS) was purchased from

12 Hybrid Plastics. Concentrated H_2SO_4 (98%), NaNO_3 , KMnO_4 , 30% H_2O_2 solution, HCl ,

13 tetrahydrofuran (THF), Na_2CO_3 , anhydrous ethanol and anhydrous methanol were all of

14 analytical grade and provided by Sinopharm Chemical Reagent Co., Ltd. (Shanghai, China).

15 DCC was obtained from J&K Chemical Reagent Co., Ltd. Epoxy resin (EP) was purchased

1 from Shanghai resin factory Co., Ltd., China. The curing agent was used
2 methylhexahydrophthalic anhydride (MeHHPA) (Yangzhou Guangrun Chemical Co., Ltd.,
3 China).

4 **2.2. Synthesis of graphene oxide**

5 Graphene oxide was synthesized from natural graphite powders according to improved
6 Hummers' methods.²⁸ Briefly, graphite powders 6 g and 3 g of sodium nitrate were added to
7 138 mL of sulfuric acid (98%) in a 500 ml beaker. At same time, an ice bath was used to keep
8 the mixture cooled down to 0°C. Then KMnO₄ (18 g) was slowly added in to the mixtures
9 and maintained the reaction temperature below 10°C. After the temperature increased to
10 35 °C and kept stirring for 7h, additional KMnO₄ (18 g) was added in the mixture, and stirred
11 for 12 h. After that, the reaction mixture was poured onto ice (800 mL) and stirred at room
12 temperature, then 30% H₂O₂ (6 mL) was added. The reaction mixture was washed with HCl
13 and deionized water, and purified by dialysis, followed by sifted, centrifuged. Finally, the
14 obtained solid was vacuum-dried overnight, obtaining 7.5 g product. The basic process was
15 shown in Scheme 1.

16 **2.3. Synthesis of ApPOSS-graphene**

17 60 mg of GO was added in 35 mL dry tetrahydrofuran (THF) in a 100 mL round-bottom
18 flask, followed 0.9 g ApPOSS and 60mg DDC (as a catalyst) was added, then dispersed by
19 sonication for 30 min. The mixture was then magnetically stirred and refluxed for 60 h at
20 75°C under nitrogen atmosphere. Every 6 h the stirring was stopped and the solution was
21 placed in an ultrasound bath for 10 min. After that, the mixture was poured into anhydrous
22 methanol (300 mL) to extract excess ApPOSS. Then the resulting mixture solutions were

1 filtered through a 0.22 μm PVDF membrane and washed with dry THF to remove the
2 residual ApPOSS. Finally, the filter cake was then vacuum-dried at 80 $^{\circ}\text{C}$. The synthetic route
3 of ApPOSS-graphene was shown in Scheme 1.

4 **2.4. Preparation of epoxy composites**

5 As shown in Scheme 1, the composites containing different filler were prepared as
6 following procedures. Typical, appropriate amounts of fillers (0.25 and 0.5 phr by weight
7 relative to the epoxy matrix) was dispersed in THF by ultrasonication for 1h and then added
8 into a stoichiometric amount of epoxy resins with stirring for 10 h and ultrasonication for 10
9 min at every 3 h. After the mixtures were got rid of THF by rotary evaporation, appropriate
10 amount of curing agent and curing accelerator were added with mechanically stirring for 30
11 min. The mixtures were repeatedly degassed in a vacuum at 80 $^{\circ}\text{C}$ about 20 min until there
12 were no trapped bubbles, then mixtures were poured into an metal mold and curing via the
13 procedures of 100 $^{\circ}\text{C}/2\text{ h} + 120\text{ }^{\circ}\text{C}/2\text{ h}$ and 150 $^{\circ}\text{C}/6\text{ h}$, respectively. Finally, the resultant
14 nanocomposites were demolded and coded EP, GO 0.25/EP, GO 0.5/EP, POSS 0.25/EP,
15 POSS 0.5/EP, ApPOSS-graphene 0.25/EP, ApPOSS-graphene 0.5/EP, where 0.25 and 0.5
16 represent the weight percent of the filler to the epoxy matrix. The general synthetic route was
17 shown in Scheme 1.

18 **2.5. Materials characterization**

19 The Fourier-transform infrared spectrum (FTIR) was conducted on a Nicolet Avatar370 FTIR
20 instrument (Thermo Nicolet, Waltham, USA). X-ray photoelectron spectroscopic (XPS)
21 measurements were performed on ESCALAB 250Xi (England). The morphology was
22 observed using a JEOL 200CX transmission electron microscope (TEM) at an acceleration

1 voltage of 200 kV. High-resolution transmission electron microscopy (HRTEM) was applied
2 to observe the SAED pattern of ApPOSS-graphene. The samples were sputtered with gold
3 and examined using scanning electron microscopy (SEM; JSM-6700F, Japan) at an activation
4 voltage of 15.0 kV. Raman spectra were recorded from 500 to 3000 cm^{-1} on a Raman
5 spectrometer (INVIA, England). The thermogravimetric analysis was performed on TA Q500
6 HiRes in a nitrogen atmosphere at a heating rate of 10 $^{\circ}\text{C min}^{-1}$ in all cases. The thermal
7 conductivities and the thermal expansion of the samples were measured by a thermal
8 conductivity tester LFA 447 Nanoflash® (NETZSCH, China) in 25 $^{\circ}\text{C}$. The surface resistivity
9 (ρ_s) and volume resistivity (ρ_v) of the materials were collected using the Agilent high
10 resistance meter 4339B (USA) and the Agilent resistivity cell 16008B (USA). In order to
11 eliminate the deviation, the measurement of every sample was conducted at least three times.

12 The volume (1) and surface (2) resistivity can be expressed as follows:

$$\rho_v = \frac{\pi \left(D_1 + \frac{B(D_2 - D_1)}{2} \right)^2}{4t} \times \frac{R_v}{10} \quad (1)$$

$$\rho_s = \frac{\pi(D_1 + D_2)}{D_2 - D_1} R_s \quad (2)$$

15 where D_1 is the main electrode (guarded electrode) diameter (mm) and D_2 is the ring
16 electrode diameter (mm), t is the average thickness of the sample (mm), R_v is the volume
17 resistance and R_s is the surface resistance, B is the coefficient of effective area and the value
18 is “1” according to ASTM D257-2014.

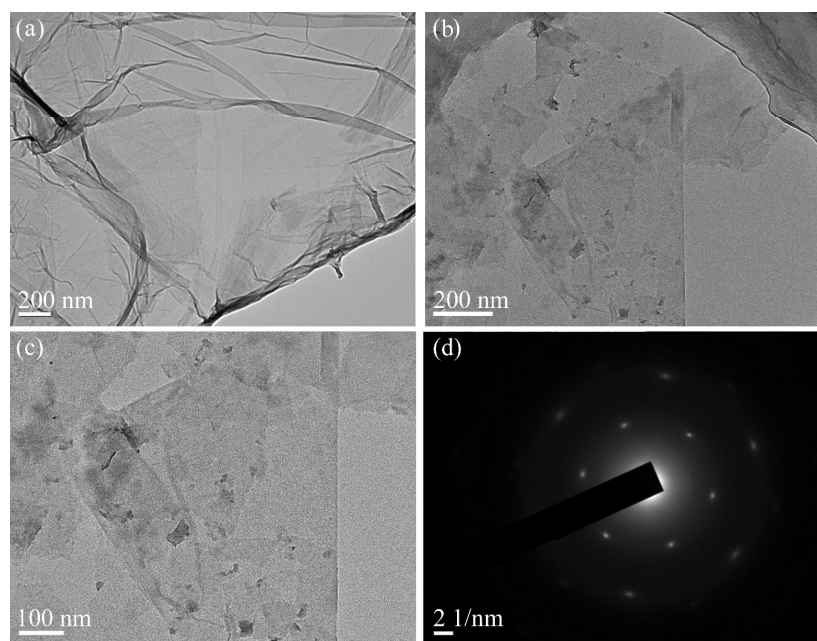
19 3. 3. RESULTS AND DISCUSSION

20 3.1. Characterization of GO and ApPOSS-graphene

21 As shown in Scheme 1a, GO was homogeneously dispersed in water, showing a color of

1 light yellow, ApPOSS as organic-inorganic hybrid materials can be homogenously dissolved
2 in THF and shows colorless (Scheme 1b). Moreover, as expected, the ApPOSS-graphene
3 displays a well dispersion in THF (Scheme 1c), indicating that ApPOSS nanomaterials are
4 successfully grafted onto GO and exhibit good organic solubility. As shown in Scheme 1d-e,
5 the neat EP and ApPOSS/EP composites show a certain transparency and the letters of the
6 background can be seen. After added GO and ApPOSS-graphene, the transparency of GO/EP
7 and ApPOSS-graphene/EP (Scheme 1f-g) is reduced.

8



9

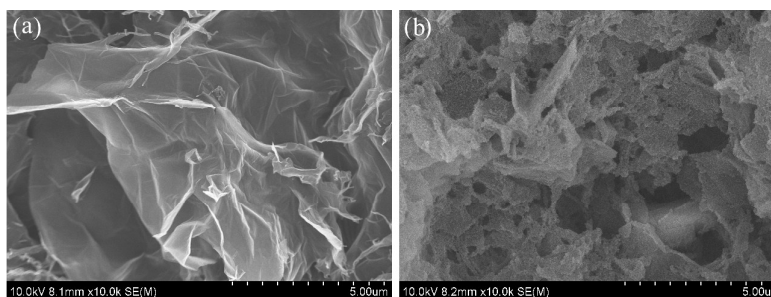
10 Figure 1. TEM images of (a) pure GO, (b, c) ApPOSS-graphene and (d) SAED pattern of
11 ApPOSS-graphene.

12

13 The TEM of ApPOSS displays regular and rectangular sheets structures (Figure S1). The
14 TEM images of GO exhibits a typically flat, laminar, wavy and wrinkled sheet structures
15 (Figure 1a), which were caused by the defects and the formation of surface functional groups

1 such as hydroxyl groups, carboxyl groups and epoxy groups. On the contrary, as shown in
2 Figure 1b-c, ApPOSS-graphene displays morphology with a flat, laminar sheet with much
3 dark spot on it, corresponding to ApPOSS, which was covalently grafted on the graphene
4 surface. In Figure 1d, the obvious six-fold symmetry structures of the selective area electron
5 diffraction (SAED) pattern of ApPOSS-graphene indicate the layered graphene structure;²⁹
6 however, the outer unresolved diffraction circles may be attributed to the grafting of ApPOSS
7 on the graphene surface.³⁰ These results also correspond to XRD analysis in supplementary
8 materials in Figure S2, which indicate that the ApPOSS are covalently grafted on GO and
9 constrain the restacking of the planar functionalized graphene nanosheets, resulting in a
10 disordered structure with low crystallinity.³¹

11



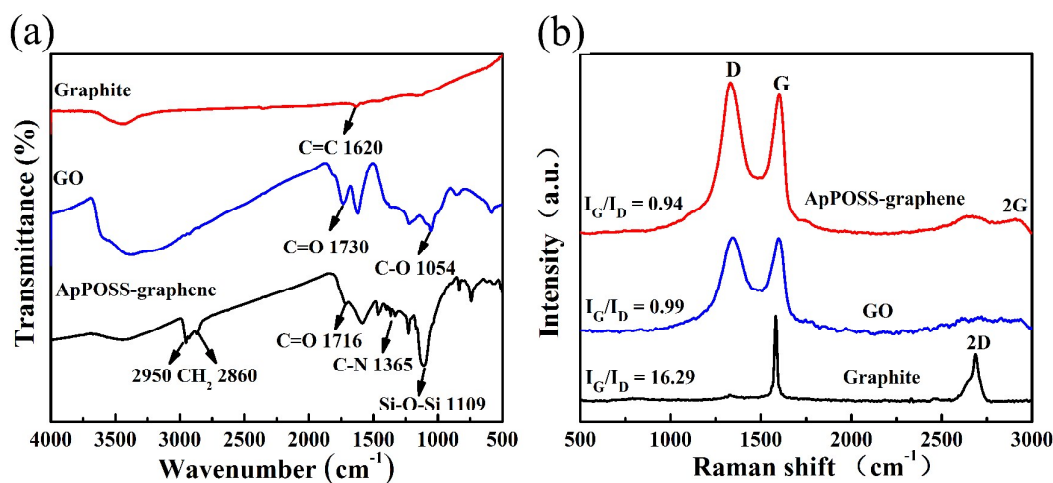
12

13 Figure 2. SEM images of (a) ApPOSS, (b) pure GO and (c) ApPOSS-graphene.

14

15 ApPOSS exhibits square block structure, in according with TEM results (Figure S1). GO
16 presents a laminar and wrinkled morphology in Figure 2a, due to its oxidation. However, in
17 Figure 2b, the ApPOSS-graphene displays coral-liked microstructure with some small
18 spheres on the surface. The roughness of ApPOSS-graphene was attributed to grafting of
19 ApPOSS on GO surface. In addition, the nucleophilic substitution between GO and ApPOSS

- 1 can cause removal of the oxygen-containing functional groups from the surface of GO
- 2 nanosheets, which could contribute to the increasing roughness of graphene sheets.³²



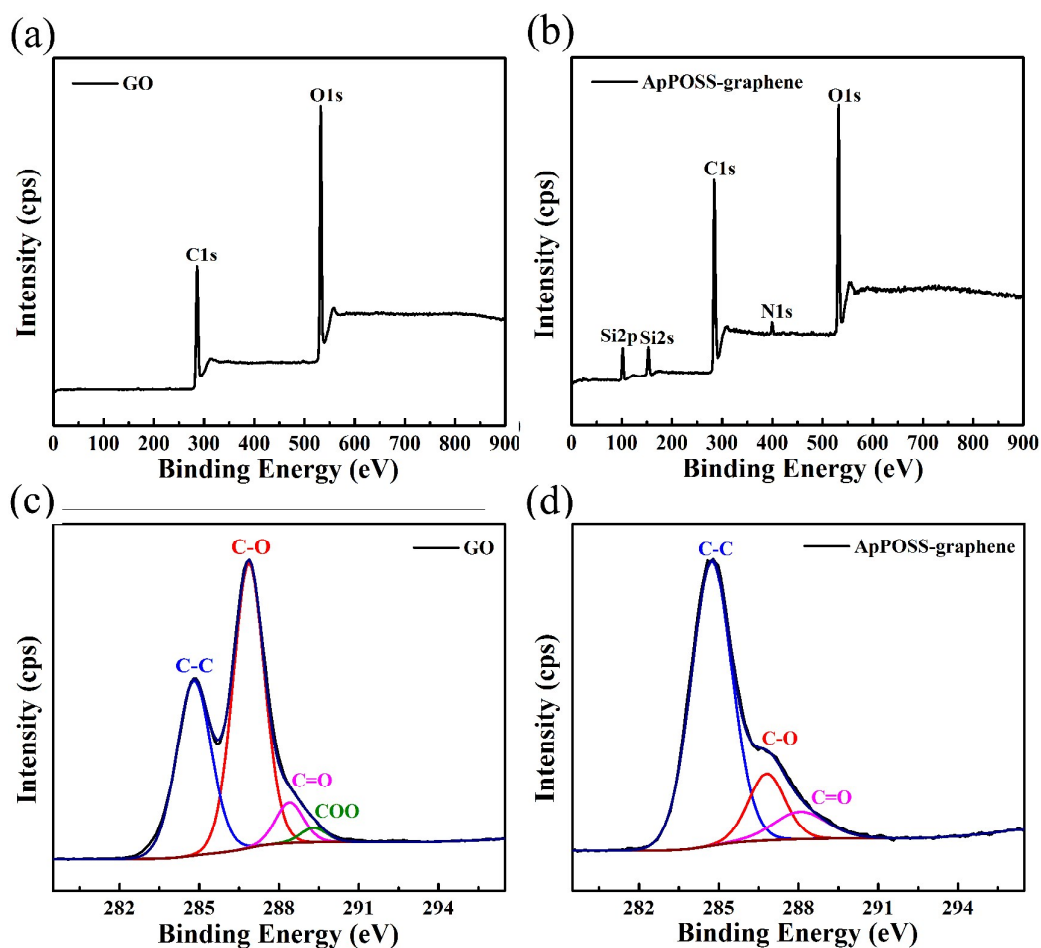
3
4 Figure 3. FTIR spectra of graphite, GO and ApPOSS-graphene (a) and Raman spectra of
5 graphite, GO and ApPOSS-graphene (b)

6
7 Figure 3a shows the FTIR spectra of graphite, GO and ApPOSS-graphene. Graphite has a
8 relatively weak bands at 1620 cm^{-1} , which are ascribed to C=C. The absorption bands of GO
9 at 3433 cm^{-1} , 1730 cm^{-1} and 1054 cm^{-1} are ascribed to hydroxyl, carbonyl groups (C=O) and
10 epoxy ring groups, respectively.^{33, 34} The absorption peaks of these groups significantly
11 decreased after ApPOSS attached onto graphene oxide through covalent binding amide
12 formation. In addition, the weak bands at 1365 cm^{-1} associated with the -C-N- groups, the
13 strong bands over $2800\text{-}3000\text{ cm}^{-1}$ associated with the isobutyl groups in ApPOSS and the
14 characteristic peak (at 1110 cm^{-1}) of the Si-O-Si were clearly seen in the IR spectrum of
15 ApPOSS-graphene, indicating that ApPOSS has been chemically grafted onto graphene. To
16 further verify the chemical modification of GO with ApPOSS, Raman spectra of graphite,
17 GO and ApPOSS-graphene are shown in Figure 1b. The Raman spectrum of the pristine

1 graphite shows a weak band at $\sim 1335\text{ cm}^{-1}$ (D band), a strong peak as the feature at ~ 1585
2 cm^{-1} (G band) and a relatively weak band at $\sim 2685\text{ cm}^{-1}$ (2D band), which are ascribed to the
3 first order zone boundary phonon mode associated with defects in the graphene or graphene
4 edges and the radial C-C stretching mode associated with sp^2 bonded carbon, respectively.³⁵
5 Graphite has a high I_G/I_D value (16.29) indicating the intact graphitic domains.³⁶ GO shows a
6 low I_G/I_D value (0.99) and unclear 2D and 2G bands, which is attributed to extensive
7 oxidation. Compared to GO, ApPOSS-graphene shows a slight small I_G/I_D value (0.94). At
8 same time, the 2D and 2G band of ApPOSS-graphene are clearly observed, due to the
9 structural distortions induced by the bulky ApPOSS “cages”. The above results indicate that
10 ApPOSS is successfully grafted onto GO surface.

11 X-Ray photoelectron spectroscopy (XPS) was employed to further explore the surface
12 chemical changes associated with the reaction shown in Scheme 1. The 17.67% of Si and
13 2.08% N content of ApPOSS-graphene suggest a successful introduction of ApPOSS. A
14 decrease of carbon and oxide content from 59.98% and 40.02% of GO to 56.55% and 23.70%
15 of ApPOSS-graphene also indicates ApPOSS grafting onto GO surface. At same time, the
16 XPS survey spectrum for GO and ApPOSS-graphene were show in Figure 4a and b. Compare
17 with GO, ApPOSS-graphene has three new peaks Si 2p (102 eV), Si 2s (153 eV) and N 1s
18 (399.5 eV), which indicate the successfulness of the covalent grafting of ApPOSS onto GO.
19 To gain further information about surface chemical changes, high-resolution XPS spectra of
20 C 1s for GO and ApPOSS-graphene were exhibited in Figure 4c and d. GO presents four
21 peaks appearing at 284.8 (C-C), 286.8 (C-O), 288.4 (C=O) and 289.3 (COOH) eV.²⁴ On the
22 contrary, in ApPOSS-graphene spectra, the COOH peak at 289.3 eV for GO almost

1 disappeared, suggesting that amide formation occurred between GO and the amine group of
 2 ApPOSS. In addition, the peak intensities of 286.5 eV (C-O) and 288.4 (C=O) eV are much
 3 weaker than those in GO, indicating that the condensation reaction between amine and GO
 4 lead to deoxygenation and reduction of GO.³⁷



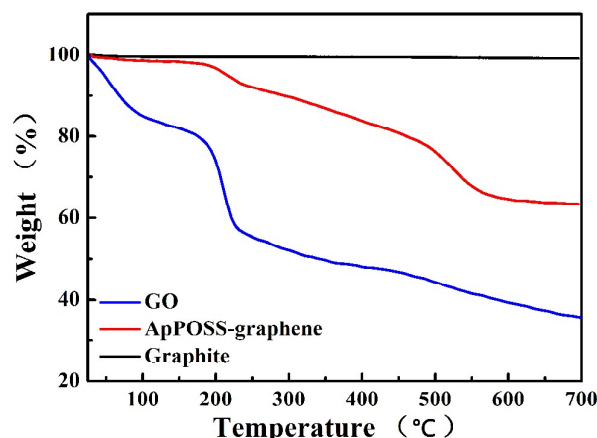
5

6 Figure 4. XPS survey spectra of the GO (a) and ApPOSS-graphene (b), high-resolution XPS

7

spectra of C 1s for GO (c) and ApPOSS-graphene (d).

8



1

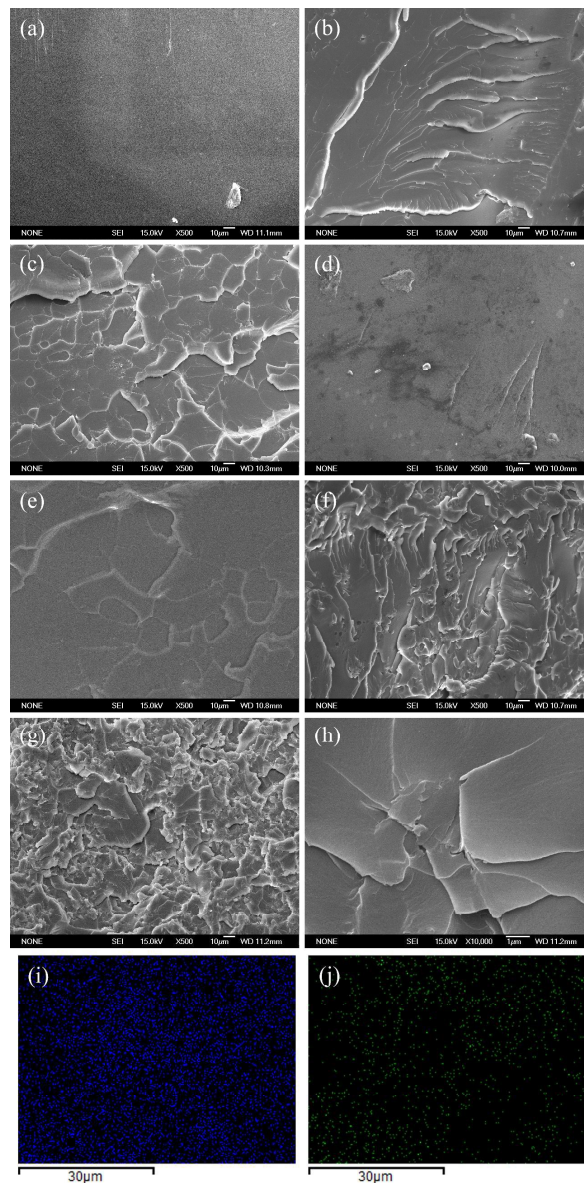
2 Figure 5. TGA curves of graphite, GO and ApPOSS-graphene with a heating rate of 10 °C
3 min⁻¹ in nitrogen atmosphere.

4

5 The thermal stability curves in nitrogen for graphite, GO and ApPOSS-graphene are show
6 in Figure 5. Graphite exhibited a simple linear dependence, with little loss, indicating its high
7 thermal stability. In contrast, GO initial weight loss below 100 °C was attributed to the
8 thermal desorption of water molecules physically adsorbed onto its hydrophilic surface. The
9 major mass loss occurring at about 200 °C was associated with pyrolysis of the labile
10 oxygen-containing groups, yielding CO, CO₂ and steam.^{38,39} Interestingly, the TGA curves of
11 ApPOSS-graphene are above that of GO at all temperature range and exhibit a new mass loss
12 stage at about 480 °C, which indicate the thermal stabilities of ApPOSS-graphene improve
13 greatly compared to GO and display more complicated thermal degradation behavior. In
14 addition, at 700 °C the weight loss of GO and ApPOSS-graphene is 63% and 37%,
15 respectively. The remarkable increase in thermal stabilities of ApPOSS-graphene is
16 associated with thermal stable cubic Si-O-Si core and amine of ApPOSS, which can react
17 with oxygen-containing groups forming amide bond and simultaneously reduce GO to
18 graphene.

1 3.2. Morphology of ApPOSS-graphene/EP

2 The morphologies of the composites from impact fracture surface were investigated using
3 SEM to research the extent of dispersion and the interfacial interactions between fillers and
4 epoxy matrix. As shown in Figure 6(a), the smooth and clean fracture surface corresponded to
5 the brittle failure of the neat epoxy resin. With the addition of fillers, the fracture surfaces of
6 composites become quite different. GO nanosheets caused rough and aggregation structures
7 with plane-like “stair” to be formed, which was due to GO hydrophilicity and poor dispersion
8 in organic solvents resulting in the formation of multi-layered stacks⁴⁰, as shown in Figure
9 6(b) and (c). The fractured cross-sections in Figure 6(d, e) were slightly rough when the small
10 cubic ApPOSS was introduced into epoxy resin. The fracture surface of GO/EP indicated that
11 there was a poor compatibility and weak interfacial interactions between fillers and epoxy
12 matrix. In contrast, the cross-sections surfaces were very rough and complicated when the
13 unique-structured ApPOSS-graphene were loaded in epoxy, the crumpled, wrinkled and
14 wave-like topology structures were seen in Figure 6(f, h), which may lead to effective
15 mechanical interlocking with the matrix.⁴¹ To further study ApPOSS-graphene distribution in
16 epoxy matrix, the EDS maps of ApPOSS-graphene 0.50/EP presents Si and N elements
17 distribution as shown in Figure 6(i, j), which suggest ApPOSS-graphene are homogeneously
18 dispersed in epoxy matrix. In addition, for ApPOSS-graphene 0.50/EP, there are no pulled-out
19 or agglomerate phenomena and it show an extraordinary difference from other systems in the
20 interfacial interaction between the matrix and fillers, indicating that ApPOSS-graphene
21 nanosheets exhibit a good dispersion, strong compatibility and interfacial interaction in the
22 epoxy matrix.



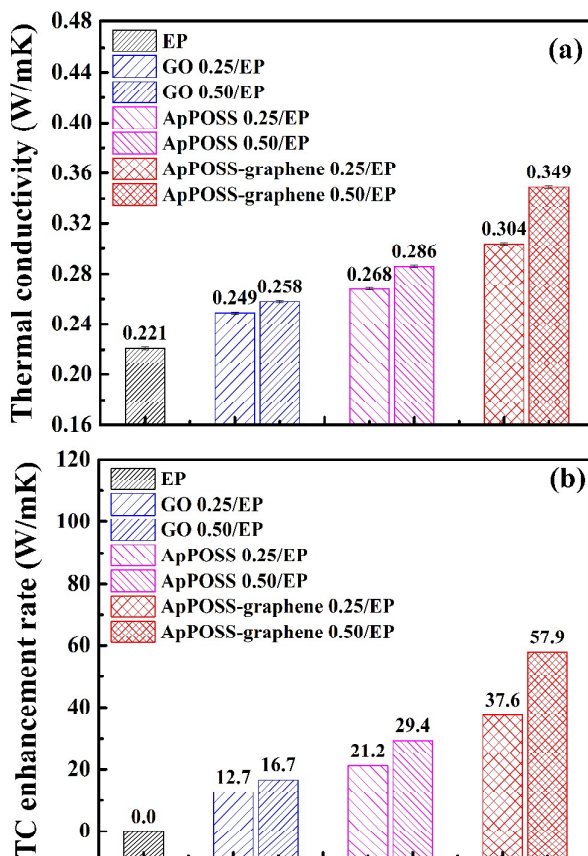
1

2 Figure 6. SEM images of fractured cross-section pure epoxy and its composites: (a) neat EP,
3 (b) GO 0.25/EP, (c) GO 0.50/EP, (d) ApPOSS 0.25/EP, (e) ApPOSS 0.50/EP, (f)
4 ApPOSS-graphene 0.25/EP, (g) and (h) ApPOSS-graphene 0.50/EP, (i) and (j) EDS maps of
5 ApPOSS-graphene 0.50/EP about Si and N elements distribution.

6

7 3.3. Thermal conductivity of ApPOSS-graphene/EP

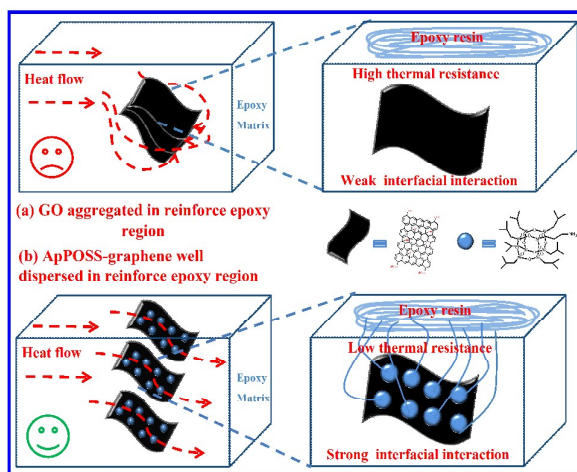
8



1

2 Figure 7. (a) Thermal conductivity and (b) its rise rate (%) of neat epoxy and its composites

3 filled with GO, ApPOSS and ApPOSS-graphene at 0.25 and 0.5 wt% loading.



4

5 Scheme 2. Schematic illustrating the heat conduct mechanism of (a) GO and (b)

6

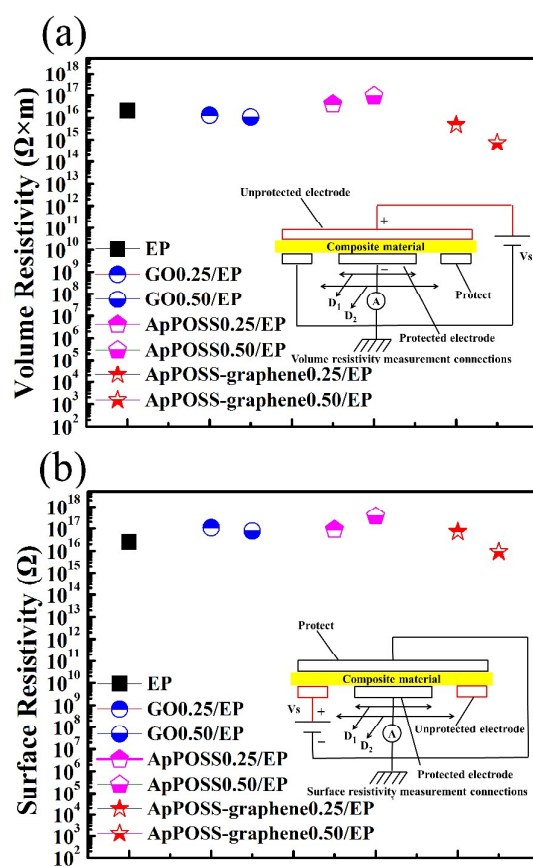
ApPOSS-graphene in epoxy resin

7

1 As shown in Figure 7a, the thermal conductivities of neat epoxy and its composites filled
2 with GO, ApPOSS and ApPOSS-graphene at 0.25 and 0.5 wt% loading were tested. It can be
3 seen that the thermal conductivity increased with the addition of filler for all three filler
4 systems tested, beginning at $0.221 \text{ W m}^{-1} \text{ K}^{-1}$ for the neat epoxy (EP), reaching 0.258 W m^{-1}
5 K^{-1} at 0.5 wt% GO and $0.286 \text{ W m}^{-1} \text{ K}^{-1}$ at 0.5 wt% ApPOSS, respectively. Compared to GO,
6 ApPOSS can be well distributed into organic solvent such as acetone, chloroform and
7 tetrahydrofuran,⁴ which contribute to its well compatibility in epoxy resin and lead to less
8 phonon transfer scattering. The thermal conductivities of ApPOSS-graphene epoxy
9 composites at 0.25 and 0.50 wt% increase by 37.6 % and 57.9 % (Figure 7b.), i.e., to 0.304
10 and 0.349 W/mK , which are more effective than GO and ApPOSS. The thermal conductivity
11 rise rate is shown in Figure 7b. We can easily know the order of thermal conductivity of the
12 three types EP composites, $\text{EP} < \text{GO/EP} < \text{ApPOSS} < \text{ApPOSS-graphene/EP}$ over the whole
13 loading range. The phenomenon may be caused by several factors. Firstly, as we know, the
14 thermal conductivity of composites is affected by filler structure, loading content, dispersion,
15 and the thermal resistance of interface between filler and composites. Even though graphene
16 has excellent thermal conductivity,⁴² it can't be well dispersed and incompatible in epoxy
17 resin, which has limited graphene effectiveness in improving the thermal conductivity of the
18 composites. ApPOSS-graphene as a novel thermally conductive and electrical insulating filler
19 can be well homogeneously distributed into organic solvent and compatible in epoxy resin,
20 which effectively decreased the interfacial thermal resistance. Secondly, as analysed in the
21 SEM images (Figure 6), ApPOSS-graphene has excellent dispersion and no aggregations in
22 epoxy matrix. Furthermore, ApPOSS-graphene formed effective thermal conduct networks in

- 1 matrix. Finally, there are many complex defects in GO, which limit its thermal conductivity.
- 2 However, the chemically converted ApPOSS-graphene eliminated defects and ApPOSS also
- 3 has good compatibility, so ApPOSS-graphene/EP composites exhibit the outstanding
- 4 performance of thermal conductivity (as shown in Scheme 2).

5 3.4. The electrical resistivity of ApPOSS-graphene/EP



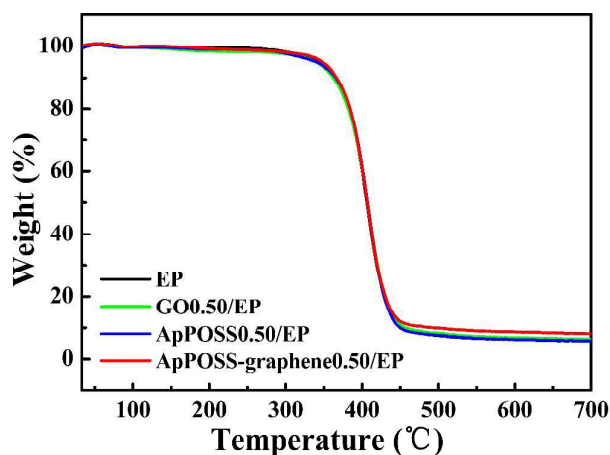
6
7 Figure 8. Volume resistivity (a) and surface resistivity (b) of EP composites with various
8 contents of fillers; Simplified illustrations are inset to explain the volume resistivity and
9 surface resistivity test setup.

10

11 High electrical resistivity is usually a desirable property in thermal interfacial materials
12 for electronic industry. To demonstrate the electrical resistivity of the neat EP and the EP

1 nanocomposite, the volume resistivity (ρ_v) and surface resistivity (ρ_s) were tested at room
2 temperature. Figure 8 shows the ρ_v and ρ_s of nanocomposites with various fillers. Adding GO
3 to the epoxy resin lead to a slight decrease of ρ_v and ρ_s , because very little π -bonds maybe
4 exist. However, with introducing ApPOSS into epoxy resin, the ρ_v and ρ_s increased, which
5 was attributed to the unique cube Si-O-Si core structure of ApPOSS. In general, adding
6 graphene to epoxy resin can effectively improve the thermal conductivity of the EP
7 composites and decrease the electrical resistivity because of graphene having large scale
8 π -bonds and high electron mobility. In contrast, the volume resistivity of
9 ApPOSS-graphene/EP composites decreases slightly compared to neat EP, while its value
10 maintains at high magnitudes. It can be seen, the resistivity (ρ_v, ρ_s) is higher than $10^9 \Omega \cdot \text{cm}$ or
11 Ω , indicating that it is an insulator and exhibits high electrical insulation properties. These
12 can be explained that the cube Si-O-Si core structures on the ApPOSS-graphene surface
13 effectively hinder the formation of electrical paths in ApPOSS-graphene/EP because the
14 ApPOSS disrupted conjugating electron transport and increased the tunneling energy barrier.

15 3.8. The thermal gravity analysis of ApPOSS-graphene/EP



16

17 Figure 9. TGA curves of EP, GO0.50/EP, ApPOSS0.50/EP and ApPOSS-granphene0.50/EP in

1 a nitrogen atmosphere.

2 TGA curves of EP, GO 0.50/EP, ApPOSS 0.50/EP and ApPOSS-graphene 0.50/EP as a
3 function of temperature are shown in Figure 9. The onset degradation temperature [T_{onset} ($^{\circ}\text{C}$)]
4 and the final char yields at 700°C are also listed in Table S1. The T_{onset} is defined as the
5 temperature at which the weight loss is 5%. As shown in Figure 9 and Table S1, the T_{onset} of
6 GO 0.50/EP is lower than neat EP, which is attributed to the thermally unstable GO and its
7 weak compatibility with epoxy matrix.³⁸ ApPOSS incorporations with epoxy resin lead to a
8 slightly decrease in T_{onset} of ApPOSS 0.50/EP compared to neat EP, due to the unstable
9 multialkyl groups in ApPOSS. However, the T_{onset} of ApPOSS 0.50/EP is higher than that of
10 GO 0.50/EP, due to that ApPOSS has unique cube Si-O-Si core structure and amino groups
11 which can react with epoxy groups. ApPOSS-graphene/EP composites exhibit the best
12 thermal stability, the T_{onset} of ApPOSS-graphene 0.50/EP has a 4.45°C increment compared
13 to that of neat EP. These can be explained that GO was reduced by ApPOSS and chemically
14 converted into ApPOSS-graphene, which improved filler dispersion, compability and
15 interfacial interaction in epoxy matrix as well as increasing crosslinking densities and
16 hindering the mobility of epoxy chains. ApPOSS-graphene 0.50/EP showed the highest char
17 yield, indicating high thermal-oxidative degradation resistance, the results approximately
18 corresponded to the thermal stability properties of chemically converted ApPOSS-graphene.
19 These were also attributed to ApPOSS grafted on graphene surface, which thermally
20 degraded to silica layers covered on sheets surface, and then created a “Tortuous path” and
21 formed a gas barrier, delaying the thermal decomposition of organic resins and reducing the
22 volatilization rate of decomposition products, finally leading to higher char yield.

1 4. CONCLUSIONS

2 A chemically converted ApPOSS-graphene nanomaterial were synthesized via the amide
3 formation between ApPOSS and GO chemical reaction. The ApPOSS-graphene has well
4 hydrophobic, it not only can disperse in many common organic solvent including chloroform,
5 acetone and THF, but also can be well compatibility in the epoxy resin. Then the
6 ApPOSS-graphene was used to modify epoxy and found that the addition of a very low
7 loading of ApPOSS-graphene with only 0.25 wt% and 0.50 wt% into epoxy matrix could
8 increase the thermal conductivity by 37.6 % and 57.9 % at room temperature. In addition the
9 ApPOSS-graphene/EP maintain a high resistivity. Therefore, ApPOSS-graphene as a novel
10 thermally conductive and electric insulation filler has a potential application in electronics
11 and microelectronic technique industry.

12 ACKNOWLEDGMENT

13 We thank the auspices from the Municipal Natural Science Foundation of Shanghai
14 2014(Grant NO.14ZR1414700), Program for Professor of Special Appointment (Eastern
15 Scholar) at Shanghai Institutions of Higher Learning (B.39-0411-10-001), Key Subject of
16 Shanghai Municipal Education Commission (J50102), the National Natural Science
17 Foundation of China (51202140), Professional and Technical Service Platform of Design and
18 Manufacture for Advanced Composite Materials, Shanghai (13DZ2292100). We thank Miss
19 Y. Zhang at Nano-Technology & Application of National Engineering Research Center for
20 SEM observations and Dr. PF. Hu and Instrumental Analysis & Research Center of Shanghai
21 University for assistance with the HRTEM measurements.

22 Notes and references

- 1 1. G. Das and N. Karak, *Prog. Org. Coat.*, 2010, 69, 495-503.
- 2 2. P. Sudhakara, P. Kannan, K. Obireddy and A. V. Rajulu, *J. Mater. Sci.*, 2011, 46, 2778-2788.
- 3 3. L. Chen, S. Chai, K. Liu, N. Ning, J. Gao, Q. Liu, F. Chen and Q. Fu, *Acs Appl. Mater.Interfaces*, 2012, 4,
4 4398-4404.
- 5 4. R. Wang, D. Zhuo, Z. Weng, L. Wu, X. Cheng, Y. Zhou, J. Wang and B. Xuan, *J. Mater. Chem. A*, 2015, 3,
6 9826-9836.
- 7 5. I. Hyungu and K. Jooheon, *Carbon*, 2012, 50, 5429-5440.
- 8 6. Q. Li, Y. Guo, W. Li, S. Qiu, C. Zhu, X. Wei, M. Chen, C. Liu, S. Liao, Y. Gong, A. K. Mishra and L. Liu,
9 *Chem. Mater.*, 2014, 26, 4459-4465.
- 10 7. C. C. Teng, C. C. M. Ma, C. H. Lu, S. Y. Yang, S. H. Lee, M. C. Hsiao, M. Y. Yen, K. C. Chiou and T. M. Lee,
11 *Carbon*, 2011, 49, 5107-5116.
- 12 8. K. S. Novoselov, A. K. Geim, S. V. Morozov, D. Jiang, M. I. Katsnelson, I. V. Grigorieva, S. V. Dubonos
13 and A. A. Firsov, *Nature*, 2005, 438, 197-200.
- 14 9. Y. B. Zhang, Y. W. Tan, H. L. Stormer and P. Kim, *Nature*, 2005, 438, 201-204.
- 15 10. A. K. Geim and K. S. Novoselov, *Nat. Mater.*, 2007, 6, 183-191.
- 16 11. S. Gilje, S. Han, M. Wang, K. L. Wang and R. B. Kaner, *Nano Lett.*, 2007, 7, 3394-3398.
- 17 12. C. Berger, Z. M. Song, T. B. Li, X. B. Li, A. Y. Ogbazghi, R. Feng, Z. T. Dai, A. N. Marchenkov, E. H. Conrad,
18 P. N. First and W. A. de Heer, *J. Phys. Chem. B*, 2004, 108, 19912-19916.
- 19 13. W. Liang, G. Zhang, H. Sun, P. Chen, Z. Zhu and A. Li, *Sol. Energ. Mat. Sol. C.*, 2015, 132, 425-430.
- 20 14. A. A. Balandin, S. Ghosh, W. Bao, I. Calizo, D. Teweldebrhan, F. Miao and C. N. Lau, *Nano Lett.*, 2008, 8,
21 902-907.
- 22 15. K. S. Novoselov, A. K. Geim, S. V. Morozov, D. Jiang, Y. Zhang, S. V. Dubonos, I. V. Grigorieva and A. A.
23 Firsov, *Science*, 2004, 306, 666-669.
- 24 16. H. Im and J. Kim, *Carbon*, 2011, 49, 3503-3511.
- 25 17. Y. Liu, X. Meng, Z. Liu, M. Meng, F. Jiang, M. Luo, L. Ni, J. Qiu, F. Liu and G. Zhong, *Langmuir*, 2015, 31,
26 8841-8851.
- 27 18. X. Cui, P. Ding, N. Zhuang, L. Shi, N. Song and S. Tang, *Acs Appl. Mater.Interfaces*, 2015, 7,
28 19068-19075.
- 29 19. N. Yousefi, X. Sun, X. Lin, X. Shen, J. Jia, B. Zhang, B. Tang, M. Chan and J.-K. Kim, *Adv. Mater.*, 2014, 26,
30 5480-5487.
- 31 20. M. N. Almadhoun, M. N. Hedhili, I. N. Odeh, P. Xavier, U. S. Bhansali and H. N. Alshareef, *Chem.*
32 *Mater.*, 2014, 26, 2856-2861.
- 33 21. Z. Wang, S. Leng, Z. Wang, G. Li and H. Yu, *Macromolecules*, 2011, 44, 566-574.
- 34 22. S. W. Kuo and F. C. Chang, *Prog. Polym. Sci.*, 2011, 36, 1649-1696.
- 35 23. K. Tanaka and Y. Chujo, *J. Mater. Chem.*, 2012, 22, 1733-1746.
- 36 24. X. Wang, L. Song, H. Y. Yang, W. Y. Xing, B. Kandola and Y. Hua, *J. Mater. Chem.*, 2012, 22,
37 22037-22043.
- 38 25. W. Q. Yu, J. F. Fu, X. Dong, L. Y. Chen and L. Y. Shi, *Compos. Sci. Technol.*, 2014, 92, 112-119.
- 39 26. L. Valentini, S. B. Bon, M. Cardinali, O. Monticelli and J. M. Kenny, *Chem. Phys. Lett.*, 2012, 537, 84-87.
- 40 27. A. Lerf, H. Y. He, M. Forster and J. Klinowski, *J. Phys. Chem. B*, 1998, 102, 4477-4482.
- 41 28. D. C. Marcano, D. V. Kosynkin, J. M. Berlin, A. Sinitskii, Z. Sun, A. Slesarev, L. B. Alemany, W. Lu and J.
42 M. Tour, *Acs Nano*, 2010, 4, 4806-4814.
- 43 29. M. A. Rafiee, J. Rafiee, Z. Wang, H. Song, Z. Z. Yu and N. Koratkar, *Acs Nano*, 2009, 3, 3884-3890.
- 44 30. T. Kuila, A. K. Mishra, P. Khanra, N. H. Kim, M. E. Uddin and J. H. Lee, *Langmuir*, 2012, 28, 9825-9833.

- 1 31. W. H. Liao, S. Y. Yang, S. T. Hsiao, Y. S. Wang, S. M. Li, C. C. M. Ma, H. W. Tien and S. J. Zeng, *Acs Appl.*
2 *Mater.Interfaces*, 2014, 6, 15802-15812.
- 3 32. J. T. Paci, T. Belytschko and G. C. Schatz, *J. Phys. Chem. C*, 2007, 111, 18099-18111.
- 4 33. J. F. Ou, J. Q. Wang, S. Liu, B. Mu, J. F. Ren, H. G. Wang and S. R. Yang, *Langmuir*, 2010, 26,
5 15830-15836.
- 6 34. C. N. R. Rao, A. K. Sood, K. S. Subrahmanyam and A. Govindaraj, *Angew. Chem. Int. Edit.*, 2009, 48,
7 7752-7777.
- 8 35. N. Wu, X. L. She, D. J. Yang, X. F. Wu, F. B. Su and Y. F. Chen, *J. Mater. Chem.*, 2012, 22, 17254-17261.
- 9 36. P. G. Song, Z. H. Cao, Y. Z. Cai, L. P. Zhao, Z. P. Fang and S. Y. Fu, *Polymer*, 2011, 52, 4001-4010.
- 10 37. M. Herrera-Alonso, A. A. Abdala, M. J. McAllister, I. A. Aksay and R. K. Prud'homme, *Langmuir*, 2007,
11 23, 10644-10649.
- 12 38. Z. Xu and C. Gao, *Macromolecules*, 2010, 43, 6716-6723.
- 13 39. B. Zhang, Y. Chen, X. D. Zhuang, G. Liu, B. Yu, E. T. Kang, J. H. Zhu and Y. X. Li, *J. Polym. Sci. Pol. Chem.*,
14 2010, 48, 2642-2649.
- 15 40. Q. H. Liu, X. F. Zhou, X. Y. Fan, C. Y. Zhu, X. Y. Yao and Z. P. Liu, *Polym-plast. Technol.*, 2012, 51,
16 251-256.
- 17 41. M. C. Hsiao, S. H. Liao, M. Y. Yen, C. C. Teng, S. H. Lee, N. W. Pu, C. A. Wang, Y. Sung, M. D. Ger, C. C.
18 M. Ma and M. H. Hsiao, *J. Mater. Chem.*, 2010, 20, 8496-8505.
- 19 42. A. A. Balandin, S. Ghosh, W. Z. Bao, I. Calizo, D. Teweldebrhan, F. Miao and C. N. Lau, *Nano Lett.*, 2008,
20 8, 902-907.

21